Mathematical Modeling of Thermal-Fluid Flow in the Meniscus Region During An Oscillation Cycle

Claudio Ojeda
Labein-Tecnalia
C/Geldo-Parque Tecnologico de Bizkaia- Edificio 700
48160-Derio(Vizcaya)-Spain
Tel.:+34-94-607-3300
Fax:+34-94-607-3349
E-mail:cojeda@labein.es

Joydeep Sengupta
University of Illinois at Urbana-Champaign
1206 West Green Street
61801 Urbana (IL)
Tel.:217-333-6919
Fax:217-244-6534
E-mail: joydeep@uiuc.edu

Brian G. Thomas
University of Illinois at Urbana-Champaign
1206 West Green Street
61801 Urbana (IL)
Tel.:217-333-6919
Fax:217-244-6534
E-mail: bgthomas@uiuc.edu

Jon Barco
Labein-Tecnalia
C/Geldo-Parque Tecnologico de Bizkaia- Edificio 700
48160-Derio(Vizcaya)-Spain
Tel.:+34-94-607-3300
Fax:+34-94-607-3349
E-mail:barco@labein.es

Jose Luis Arana
University of Basque Country
C/Alameda de Urkijo S/N
48013-Bilbao(Vizcaya)-Spain
Fax:+34-94-601-4180
E-mail:jl.arana@ehu.es

Key words: Mold powder, Lubrication, Overflow, Slag rim, Fluid flow, Consumption, Heat flux, Oscillation, Mechanism

INTRODUCTION

In continuous casting of steel, initial solidification and behavior of the meniscus are controlled by many phenomena such as the velocity of the mold, velocity of the steel, pressure field, temperature, delivery of superheat and the changes in this behavior during each oscillation cycle[1, 2]. These meniscus phenomena are important because they control molten slag consumption, lubrication, the formation of oscillation marks, subsurface hooks, and surface defects[3-8]. As an initial step in quantitative understanding of these phenomena, a computational flow model has been developed to simulate transient behavior in the meniscus region during an oscillation cycle, including fluid flow evolution in the molten slag and molten steel, movement and overflow of the steel-slag interface, slag consumption into the gap, and the effects of movement of the solid slag rim above the meniscus. In addition, a coupled heat transfer model with temperature-dependent properties is developed to predict temperature and heat flux in the meniscus region. The results quantify the fluctuations in the pressure field that in turn greatly affect the flow of liquid slag, the shape of the meniscus and the formation of oscillation marks. This work helps to understand the mechanism of formation of surface defects and quality problems in the cast product so that improvements can be found.

Surface Quality Problems

The majority of surface defects in the continuous casting process originate at, or within the first millimeter of the meniscus in the mould[9, 10]. Oscillation marks, and the associated subsurface hooks in low carbon steels, can entrap mold powder, inclusions, bubbles, and other impurities that lead to subsequent surface defects. Oscillation marks cause local nonuniformities in mold heat transfer and are common sites for crack formation.[1, 5] Surface cracks in continuously cast slabs that start at the meniscus include broad face longitudinal, transverse and star cracks, transverse corner and off corner cracks and narrow face transverse cracks. These are associated with poor mold powder consumption behavior and uneven mold heat transfer[9]. Whether the defects develop into cracks depends on heat transfer and events down the reminder of the mold and below mold exit[11, 12]. Continuous casting mould powders are being developed constantly to help improve surface quality, ensure plant safety from breakouts, enable faster casting speeds and meet with tightening environmental constraints. Most continuous casting operators continually review mold powder selection to ensure optimum performance[13-16].

Thus, it is important to understand meniscus behavior, slag infiltration into the gap, and how oscillation marks form. Many different possible mechanisms have been proposed for oscillation mark formation. These include: 1), overflow of the liquid steel over the frozen meniscus in the top of the steel shell[1], 2) overflow of the liquid steel over the solidified steel meniscus and remelting of the frozen meniscus[4, 6] and 3) bending / unbending of the weak solidified steel shell[17,18]. Fundamental understanding of defect formation requires taking into account all the different phenomena that take place at the meniscus, including the formation of the oscillation marks and slag movement.

Phenomena and Process Description

Phenomena involved in the formation of the oscillation marks include the fluid flow of the steel[1, 17, 20], transport of superheat to the meniscus region[12, 21], heat transfer from the steel to the mold[22, 23], the solidification and melting behavior of the mold powder[22], the motion of the steel / slag interface including surface tension and ferrostatic pressure forces. Of great importance is the effect of the solid slag rim that solidifies against the mold wall on the meniscus behavior[1, 6, 24].

Phenomena related to the slag rim and liquid flux flow and consumption are complex. First the powder is spread over the free surface of the steel on the top of the top of the mold. The powder particles sinter together, reject gas bubbles, and melt to form a molten slag layer in contact with the top surface of the molten steel. Some of this molten slag solidifies against the mold wall forming a solid slag rim that moves with the mold wall. Its size depends on powder properties and flow conditions at the meniscus, such as level fluctuations. The oscillation of the mold and the buoyancy of the molten slag cause flow in the region formed between the mold, the flux rim, the steel shell and the steel meniscus. The infiltration of the slag into the gap between the shell and the mold is caused mainly by the pumping effect created by the oscillation of the mold, and drag by the moving steel shell. It is widely believed that during the negative strip time, the positive pressure generated in the meniscus region pumps molten slag into the gap. On the other hand, during the positive strip time, the increasing distance between the meniscus and the solid slag rim draws molten slag into this region and so consumption correlates with the positive strip time. The rate of flux consumption has a great effect on mold heat transfer, lubrication to prevent sticking of the shell to the mold, and associated surface defects[2, 12].

Proposed Work

Mathematical models together with plant data are key tools to understand meniscus behavior and how oscillation marks form. Several previous models have been applied to investigate several of these phenomena independently[3,4,5,12,17,18,21,22,25,29]., including meniscus motion[30] during the oscillation cycle and fluid flow and pressure fluctuations in the gap[5]. The objective of this study is to advance quantitative understanding of the meniscus region phenomena by simulating fluid flow evolution in the molten slag and molten steel, movement and overflow of the steel-slag interface, slag consumption into the gap, and the effects of movement of the solid slag rim above the meniscus. A coupled heat transfer model is used to quantify the heat delivered to the mold, the temperature field and the melting behavior of the rim.

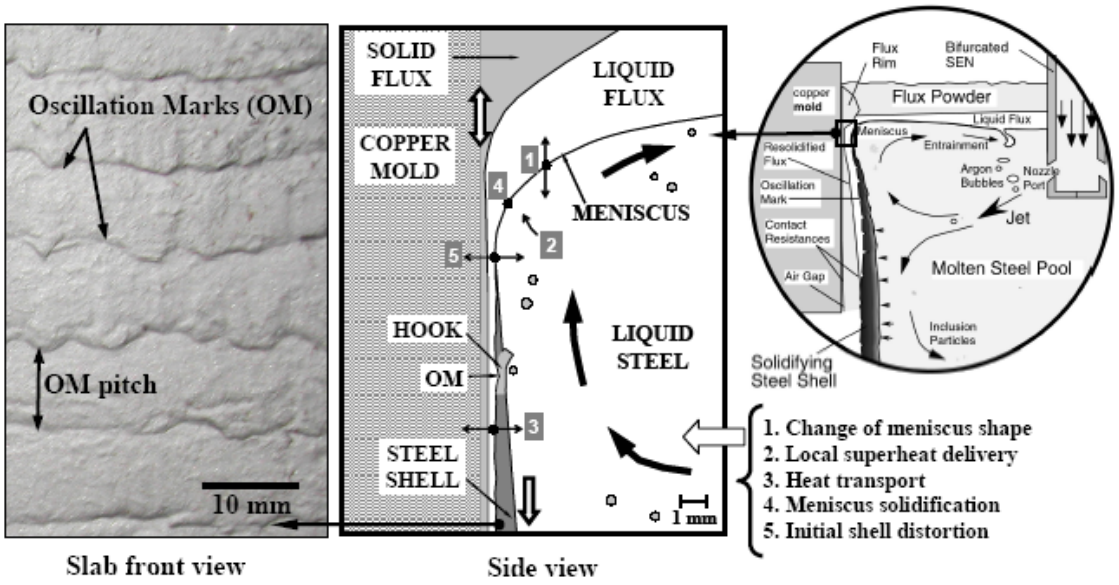

Fig. 1 Description of phenomena in meniscus region[24]

DESCRIPTION OF THE MODELS

A two dimensional computational flow model has been developed to study the fluid flow of the liquid slag, the behavior of the steel/slag interface, the consumption of slag into the gap between the steel shell and the mold, the evolution of the pressure field with time and the heat transfer in the meniscus region. The shape of the solid slag rim and solidified slag layer against the mold wall is assumed, based on previous work[1], and oscillates with the mold. The thickness of the liquid slag layer between the solidified steel shell and the solid slag layer near the shell tip is assumed to be 0.2mm, based on calculations using the CON1D model[1] for the same conditions and properties. A wedge-shaped steel shell moving down at casting speed is assumed. Superheat in the region is assumed to be high enough to prevent undercooling and meniscus freezing. The molten steel is assumed to be relatively stagnant, moving only due to the inertial forces caused by mold oscillation. The constant fluid properties are given in Table 1.

To fluid flow model solves the Navier-Stoke's equations with the k-e model for turbulence and the Volume of Fluid model to track the air, slag and steel phases and motion of their interfaces, using the commercial computational fluid dynamics (CFD) package FLUENT. The simulation domain contains powder, liquid slag and molten steel, with the solid slag layer and solid steel shell as boundaries, as shown in Fig. 2. A deforming mesh is used to incorporate the changes to the domain shape caused by oscillation of the solid rim. The boundaries of the domain are treated as walls except the top surface which is a pressure inlet with a gauge pressure of 0 Pa, the outlet of the gap which is a pressure outlet (at 0 Pa) and the right side which is a symmetry condition. This flow model is first run with no movement in the mold wall and with zero casting velocity until a steady-state is reached, meaning that the results are unchanged with time. This requires about 1.5s simulation time. Then the oscillating movement of the mold wall and the downward casting speed of the solid shell are imposed to match typical casting conditions[1] (Table 2) and the model is run to simulate over one oscillation cycle. Two runs were made. The first starts the oscillation cycle at the maximum upstroke velocity and the second starts at the maximum downstroke velocity.

Table 1 Properties of Steel and slag included in the model

Density of steel	7000 kg/m^3
Viscosity of steel	0.063 Poise
Density of slag	2500 kg/m^3
Viscosity of slag	2.62 Poise
Surface tension	1.6 N/m
Contact angle	60 deg

Table 2 Oscillation parameters and casting speed

Casting speed	1.42 m/s
Frequency	155 cpm
Stroke	6.34 mm

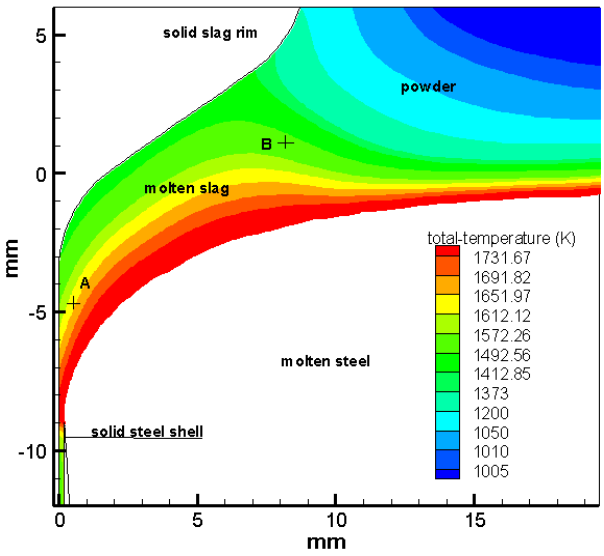

Fig. 2 Temperature field of the mold slag in the meniscus region

The heat flow model is run from the steady solution of the fluid flow model to calculate the heat delivered into the mold, the temperature field and the melting rate of the solidified slag under time-averaged conditions. In this case, the powder / slag viscosity and conductivity change with temperature according to McDavid and Thomas[22]. For boundary conditions, the solidification temperature of the slag (1374K) is imposed at the liquid slag / solid slag interface and decreases to ambient temperature from the nose of the solid rim to the top of the powder layer. The liquidus temperature of the molten steel (1805.9K) is imposed at the liquid slag / molten steel interface, and the solidus temperature (1793.9K) at the cold side of the steel shell tip. Ambient temperature is imposed at the air boundaries above the powder layer. The domain, shown by colored results in Fig. 2, is the same as that for the fluid flow model, except that temperature variations in the molten steel are not calculated.

MODEL VALIDATION

To validate the CFD model, a test case is run where an analytical solution is available. In this "stagnant" case, there is no movement of the mold wall and the solid slag rim is not included. The computed slag phase fraction contours are shown in Fig. 3, which reveal the the interface between the liquid slag (red) and the molten steel (blue). The meniscus shape is also calculated using the Bikerman equation[5] (1), which is derived by balancing the pressure forces at each side of the interface and the capillarity forces from surface tension:

$$x = -\sqrt{2a^2 - y^2} + \frac{\sqrt{2a^2}}{2}\ln\left(\frac{\sqrt{2a^2} + \sqrt{2a^2 - y^2}}{y}\right) + 0.3768a \qquad (1)$$

Where:

$a^2 = \dfrac{2\sigma}{g(\rho_s - \rho_f)g}$ is the capillary constant

x: distance form the closest point of the interface to the mold
y: vertical distance from the highest point of the interface liquid steel – liquid slag
σ: interfacial tension
ρ_s: density of the steel
ρ_f : density of the liquid mold flux
g: acceleration of gravity

Fig. 4 compares the meniscus shape for this stagnant case from both models. The shape depends on the head of unsupported liquid (given by the far-field metal level) above the tip of the solidified shell. The comparison shows that the CFD model is able to match the analytical solution exactly, even in the lower part of the Bikerman solution curve, where the unsupported liquid bulges slightly over the edge of the shell tip.

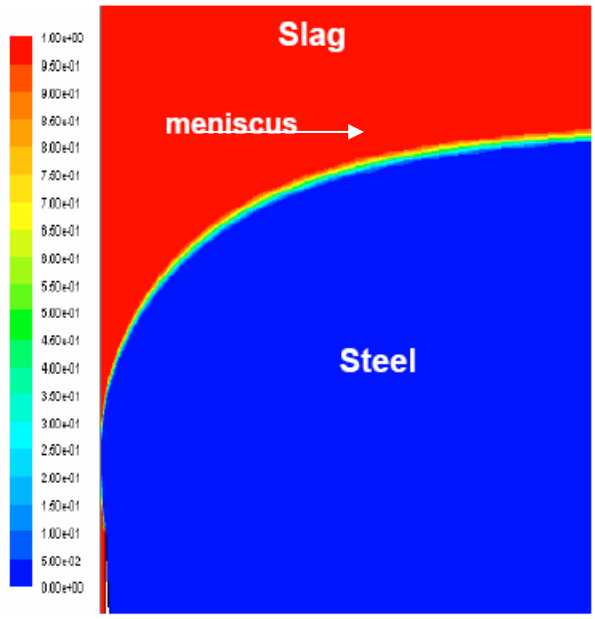

Fig. 3 Interface shape at equilibrium (flow model)

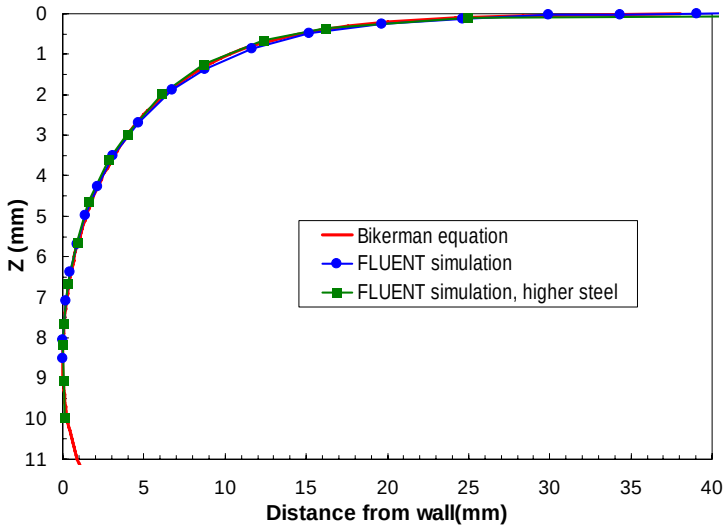

Fig. 4 Meniscus shape comparing Bikerman and flow model

RESULTS

The validated model was next run for transient conditions during an oscillation cycle, under the important influence of the moving flux rim. The oscillation cycle, illustrated in Fig. 5, governs the movement of the attached slag rim and was chosen to mach conditions where measurements where available[1]. Figures. 6-14 show the velocity vectors of the fluid flow in the meniscus region colored with the phase fraction. Red arrows designate slag and blue is steel. Figure 15 summarizes schematically the key events in the flow pattern during the oscillation cycle. Figures. 16 and 17 show the velocity at points A and B (located in Fig.2). Finally Fig. 19 shows the pressure variation at a point in the liquid slag in the mold / shell gap located 16 mm below the meniscus.

In presenting the results, the oscillation cycle starts arbitrarily at time 0.00 seconds when the mold is at its equilibrium position, (matching the far-field metal level) and is moving upward at its maximum speed. The mold reaches its peak height (zero velocity) at 0.097s. Soon after starting downwards, the mold speed exceeds the casting speed, (0.125s) which starts the 0.135s-long "negative strip time". Negative strip is needed to prevent sticking of the shell to the mold. The positive strip time comprises the rest of the oscillation cycle, and starts at 0.261s. The entire cycle ends at the equilibrium position again at 0.387s.

During the first part of the oscillation cycle, when the mold is moving upward, liquid slag is flows towards the slag rim to fill the space opened as the rim moves upward, as shown in Fig. 6. Liquid slag is also drawn upward out of the gap between the steel shell and the solid slag layer due to the negative pressure generated by this upwards movement of the mold. This behavior continues until 0.06s. During the positive strip time, the interface between the liquid steel and the liquid slag is pulled towards the mold wall.

At 0.06s the liquid slag first starts to flow towards the mold wall, as shown in Fig.7. At this time, the molten steel starts to overflow the meniscus and flow into the gap between the solid slag and the solid steel shell. Even after the mold starts downwards (Fig. 8), the momentum of the steel continues to move the interface towards the mold wall.

Soon after the negative strip time starts, (Fig. 9), the molten steel has completely overflowed the meniscus, finishing at ~0.15s. The downward movement of the slag rim causes a sharp increase in positive pressure (Fig. 17). This prediction is qualitatively consistent with the mechanism of Sengupta[1], and with the computations of Takeuchi [5]. The pressure starts to push molten slag out of the region between the solid slag rim and the interface in both directions: into the shell / mold gap (where it provides lubrication consumption) and towards the center of the mold. The new slag / steel interface, which is established after the overflow, is pushed further away from the mold wall.

During the negative strip time, liquid slag is pushed into the gap, which increases the consumption rate of liquid slag as shown in Fig. 20. However, the movement of the solid slag rim downwards creates a force against the interface between the liquid steel and the liquid slag. This pushes the slag out of the meniscus region at relatively high velocity (Fig. 11). This flow pattern continues during the negative strip period and the downward movement of the mold until 0.29s. The interface shape continues to move away from the mold wall during the downward movement of the mold, except for the overflowed steel that remains in the shell / mold gap and would solidify.

During the upward movement of the mold, (Fig. 13), the results show again that the liquid slag is flowing out of the gap between the solid slag and solid steel shell and the direction of the flow in the meniscus region under the solid slag rim is towards this solid rim. The pressure during this period decreases and the flow pattern changes and goes against the solid rim into the meniscus region. During this period the interface starts to move toward the mold wall again. At the end of the first cycle, the results are almost the same as the results at 0.01s, which shows that the model is at pseudo-steady state: at the same point in the oscillation curve, the same results are predicted.

Summary of meniscus flow in an oscillation cycle

As shown schematically in Fig.15, during the positive strip time (until 0.06s), upward movement of the slag rim opens up the space above the meniscus and draws in liquid slag. Slag consumption into the gap between the steel shell and the mold is negative, and the meniscus is pulled towards the mold. Just before negative strip starts, the meniscus overflows the top of the shell. After this point, there is positive slag consumption into the gap (see Fig. 20). During the negative strip time, downward mold movement generates positive pressure and squeezes slag out of the shrinking meniscus region. Also during this period, the overflowed steel solidifies in the mold / shell gap, while a new meniscus forms and is pushed away from the mold. As the positive strip period begins again, the pressure decreases and the slag again flows beneath the rim and pulls the interface towards the mold.

Upward vertical (y) velocity near the gap inlet (point A in fig.2) increases greatly during the positive strip time, as shown in Fig. 16 This prediction agrees with experimental observations by Tsutsumi et al.[5, 25] At the same time, horizontal (x) velocity at a point far from the gap (point B in Fig. 2) is towards the slag rim, (negative), as slag flows into the meniscus region. Later, during negative strip, horizontal velocity at this point reverses, illustrating how fast the liquid slag is squeezed out.

The flow model predicts meniscus overflow starts at ~ 1/6 of the oscillation cycle before the start of the negative strip time. Running the model for more than one oscillation cycle again predicts an overflow event at the same time as in the previous oscillation. Starting the simulation case from a different point in the oscillation cycle (the time of maximum downstroke velocity) produced overflow event starting later during the negative strip time and continuing during the positive strip. Continuing this case for another cycle, the second overflow event starts at ~1/6 of the oscillation curve before negative strip, as before. This result shows that although the overflow event is consistent for a given set of conditions, minor changes in the changes, such as caused by level fluctuations or a different flux rim shape can make overflow occur at a different time in the cycle.

Slag Consumption

The instantaneous and mean consumption rate of liquid slag into the gap between the solid steel shell and the mold are shown in Fig. 20. Positive consumption starts when the overflow event drives both liquid slag and molten steel into the gap, where it is captured within the newly-formed oscillation mark. Positive consumption continues during the negative strip time, as pressure from the downward movement of the slag rim pushes slag into the gap. Positive consumption continues into the positive strip period until 0.32s, as shear stress from the downward moving steel shell drags in the liquid slag. Negative consumption (slag leaving the gap) occurs only during that part of the positive strip time that the mold is moving upwards at its maximum velocity.

The net result is that there is a positive mean consumption into the gap of 0.0053 kg/ms, (2.07 g/m/cycle) which is close to the consumption rate of 0.0058kg/ms (2.25 g/m/cycle) measured in the steel caster for the same operational data by Shin et al.[25]. The overflow event has only a minor effect on distorting the consumption curve, which is otherwise a sinusoidal curve consistent with previous work[5,25]. The model slightly under-predicts the consumption because the slag captured in the oscillation marks is neglected. Solidification of the overflowed steel and the accompanying formation of the oscillation mark shape is not included in this model. These disruptive effects of the overflow event are expected to have a more severe effect on slag consumption.

Heat transfer model

The heat transfer model results the time-averaged temperature distribution of the mold powder and liquid flux in the meniscus region, in Fig. 2. The interface between these two layers (identified by the 1373K isotherm) curves up to meet near the nose of the slag rim. It shows that the liquid slag layer is more extensive near the meniscus under the solid rim, due to the convective mixing and lower viscosity of the hot liquid flux. Only a thin liquid layer (~2mm thick) is predicted on the far left of the domain, representative of most of the top surface. This is thinner than measured, likely due to the model neglect of high-speed turbulent flow in the liquid steel pool induced by the nozzle.

The model results were further analyzed to determine the heat flux to the solidified flux layer on the left side of the domain, which then enters the water-cooled mold wall. The profile, given in Fig. 21, shows that the maximum heat flux peak is about 8mm below the liquid level (far-field meniscus), which is consistent with experimental observations. This figure also slows the corresponding melting rate of the solidified slag rim, which averages ~0.5mm/s over the lower portion of the rim for these conditions. This non-zero value means that the rim is in a non-equilibrium position relative to the interface, which can happen when there is a level rise of the steel level in the mold. These results suggest that remelting back of the rim would take less than a minute to reach a new equilibrium shape. The results here also suggest that the assumed large rim shape likely produces more pressure and other disruption of the meniscus flow during each cycle than would usually occur. Thus, the overflow event predicted here might be different than usually encountered for these oscillation conditions.

Mechanism of hook formation and shape

These model results give new insight into the mechanism for hook and oscillation mark formation. Alternating pressure due to mold oscillation and interaction with the solidified flux rim causes meniscus motion, and overflow just before the negative time starts, although the results suggest that overflow could happen at various times during the oscillation cycle. If the molten steel in the region becomes supercooled, the meniscus could solidify at some time during the cycle before overflow, leading to hook formation. Thus, the different shapes of the interface (meniscus) predicted at different times in the cycle are compared in Fig. 18 with hook shapes measured in samples from a real caster.[5, 25] The predicted range agrees remarkably well with the measurements. The curvatures also agree well, although there appears to be slightly more curvature in the measured hooks. This suggests that other phenomena, such as level fluctuations or thermal distortion may have altered the hook shape.[1] Thermal distortion is the most likely explanation, however, as the heating provided from the molten steel to the outside of the hook during overflow would cause it to expand and distort, increasing its curvature from the predicted shape of the meniscus to that observed in the solidified hook.

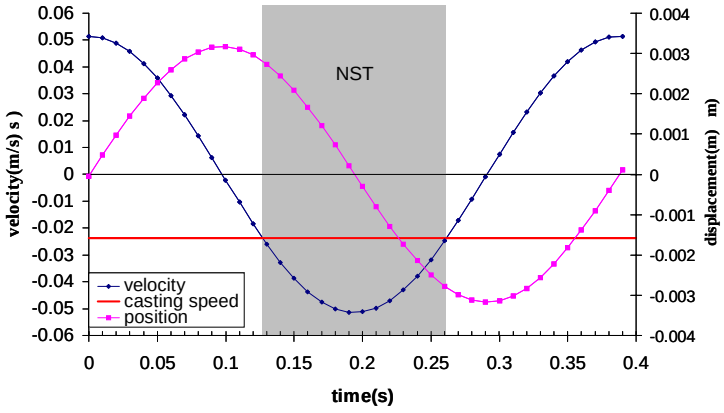

Fig. 5 Velocity and position curves during an oscillation cycle

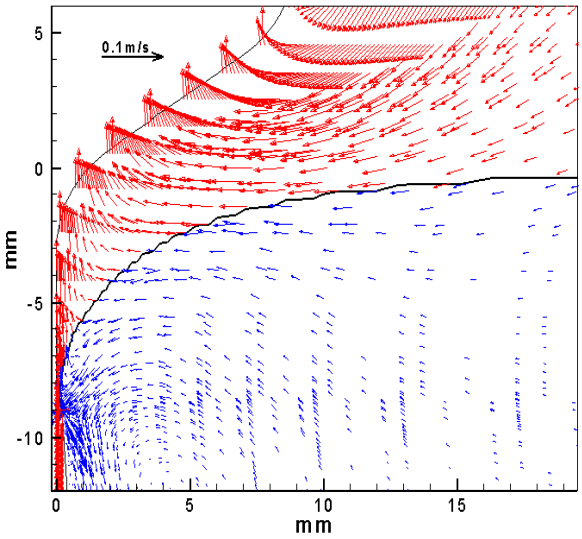

Fig. 6 Velocity vectors and interface shape at 0.01s.

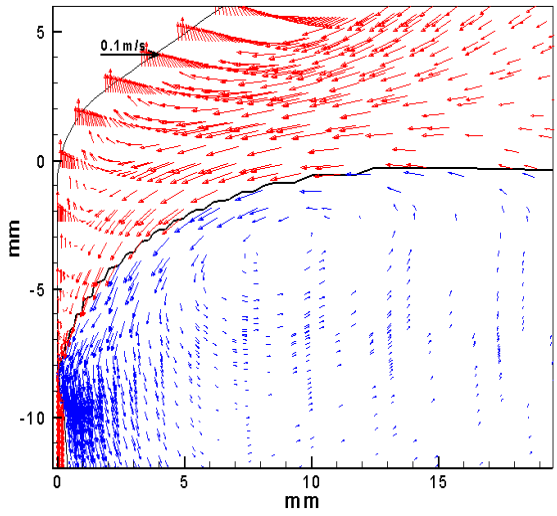

Fig. 7 Velocity vectors and interface shape at 0.06s.

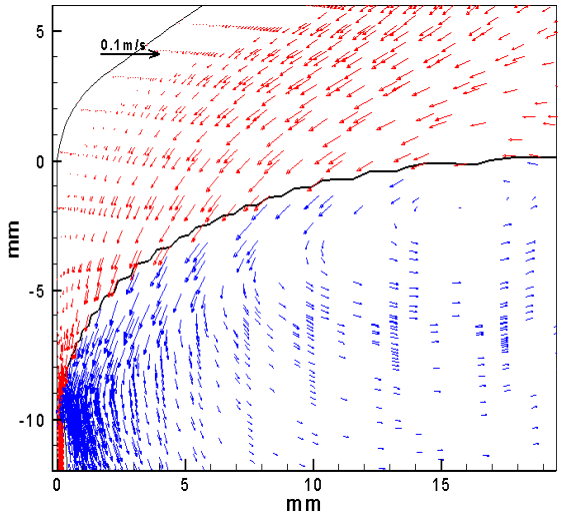

Fig. 8 Velocity vectors and interface shape at 0.10s.

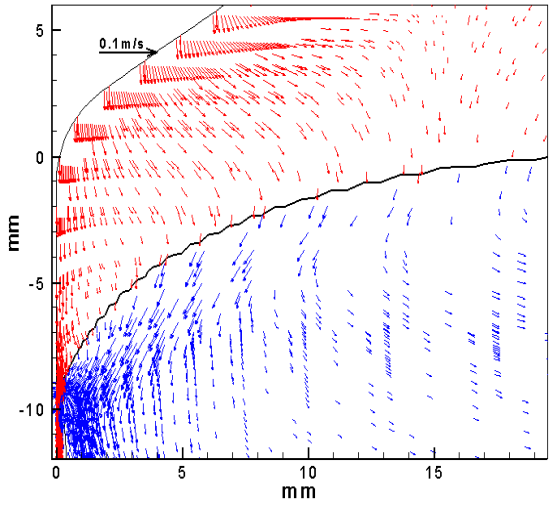

Fig. 9 Velocity vectors and interface shape at 0.14s.

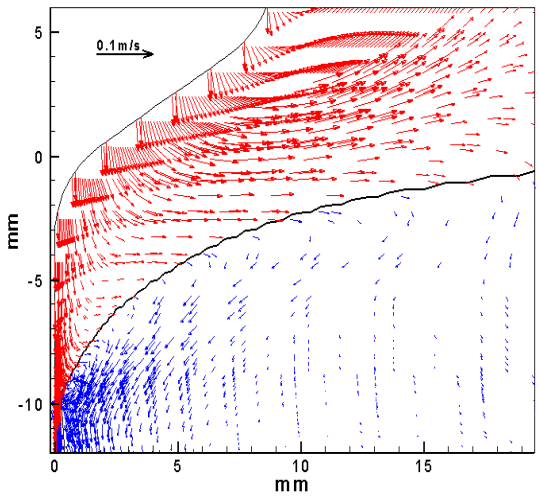

Fig. 10 Velocity vectors and interface shape at 0.19s.

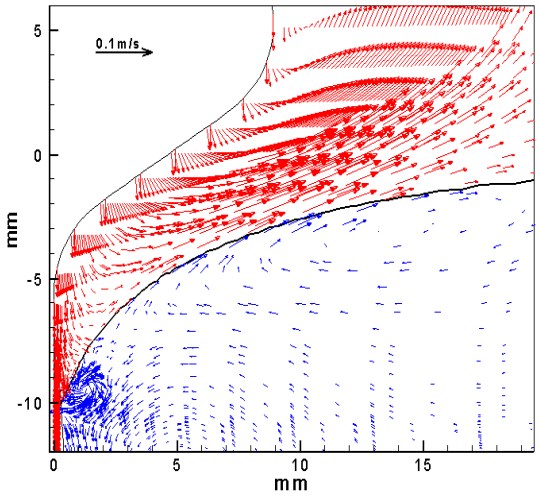

Fig. 11 Velocity vectors and interface shape at 0.24s.

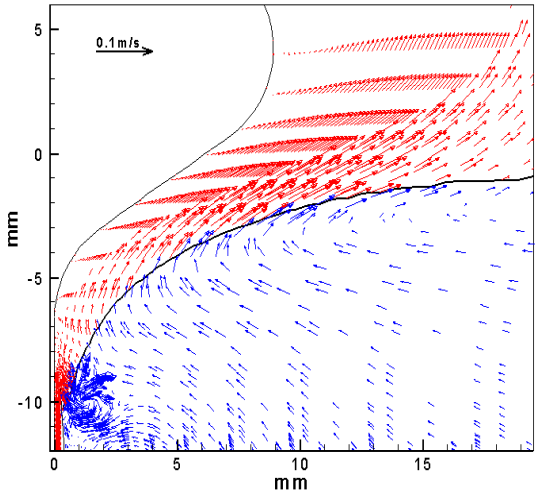

Fig. 12 Velocity vectors and interface shape at 0.29s.

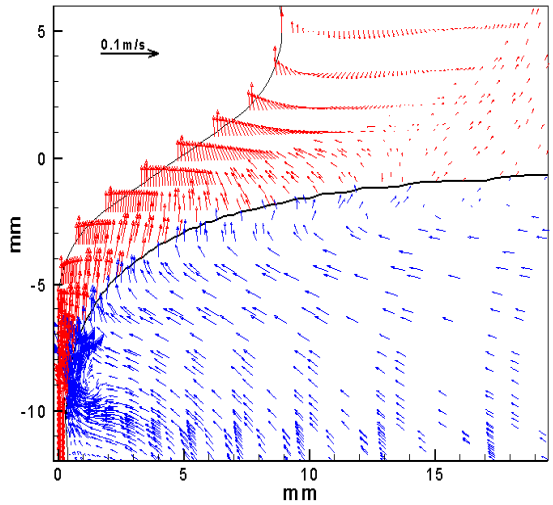

Fig. 13 Velocity vectors and interface shape at 0.34s.

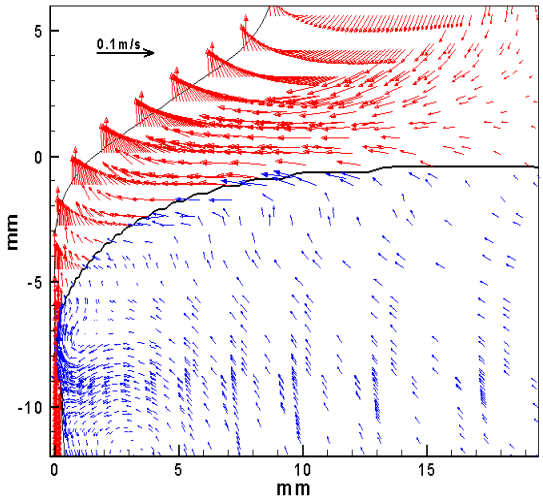

Fig. 14 Velocity vectors and interface shape at 0.39s.

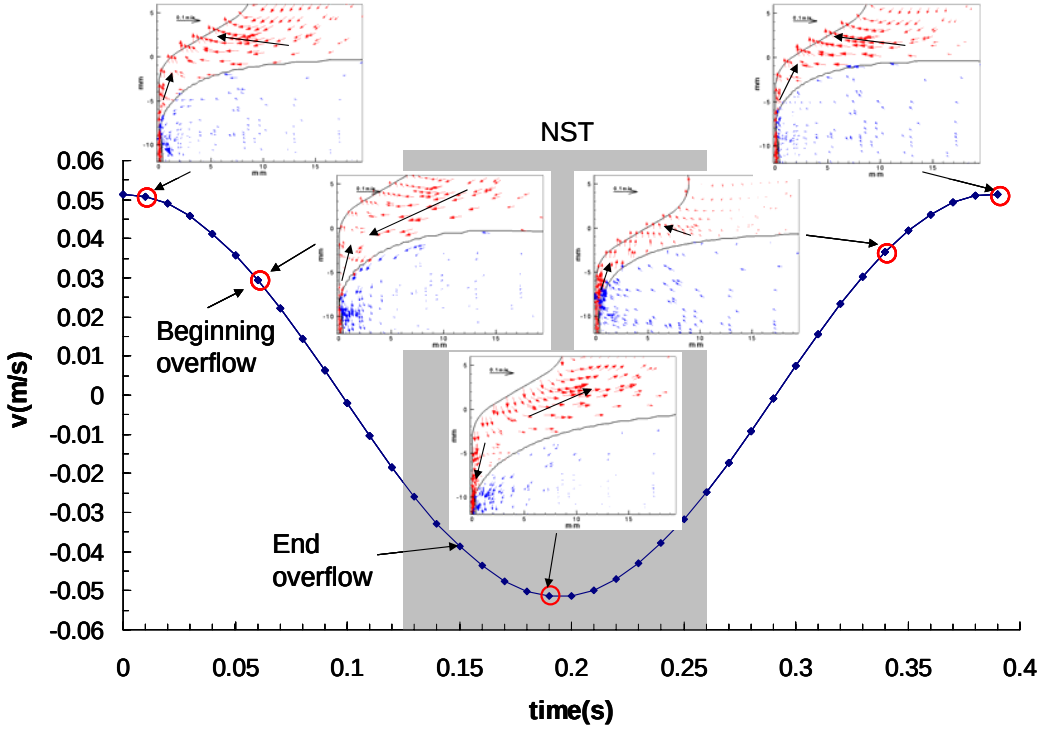

Fig. 15 Meniscus shape evolution during one oscillation cycle

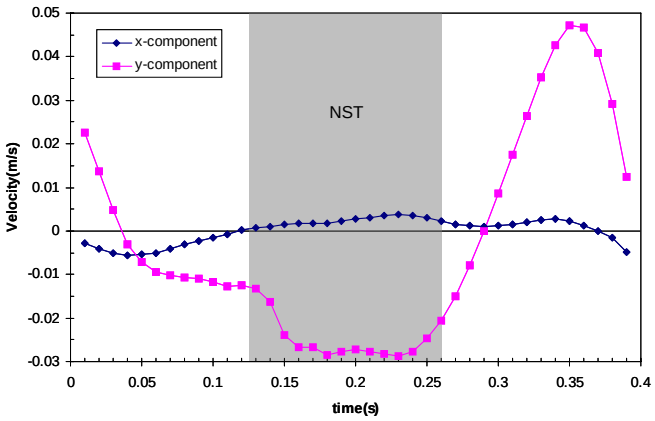

Fig. 16 Velocity components at point A (fig.2) near gap inlet

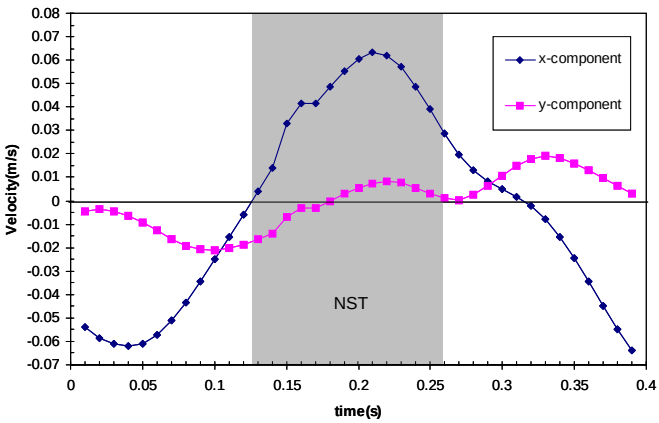

Fig. 17 Velocity components at point B (fig.2) near the solid rim nose far from gap inlet

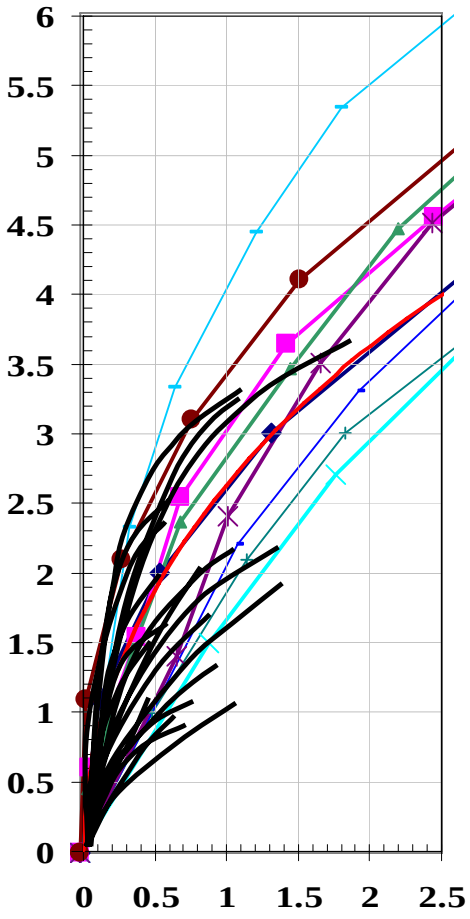

Fig. 18 Comparison of interface shapes from flow model and measured hook shapes from [1]

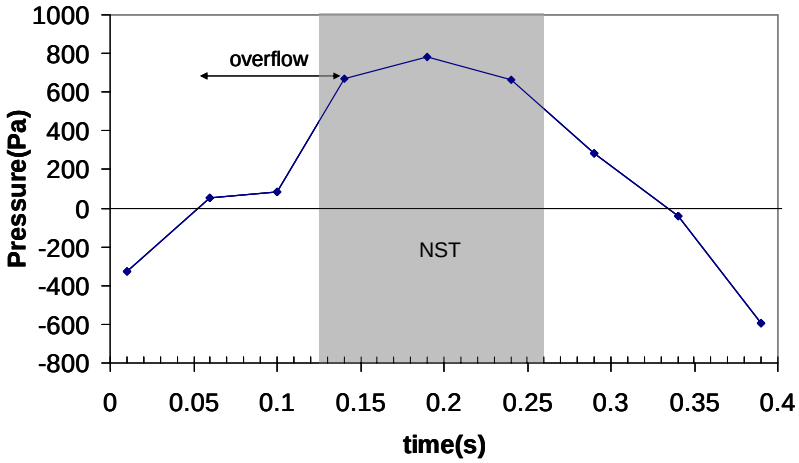

Fig. 19 Pressure in mold / shell gap 17 mm below meniscus

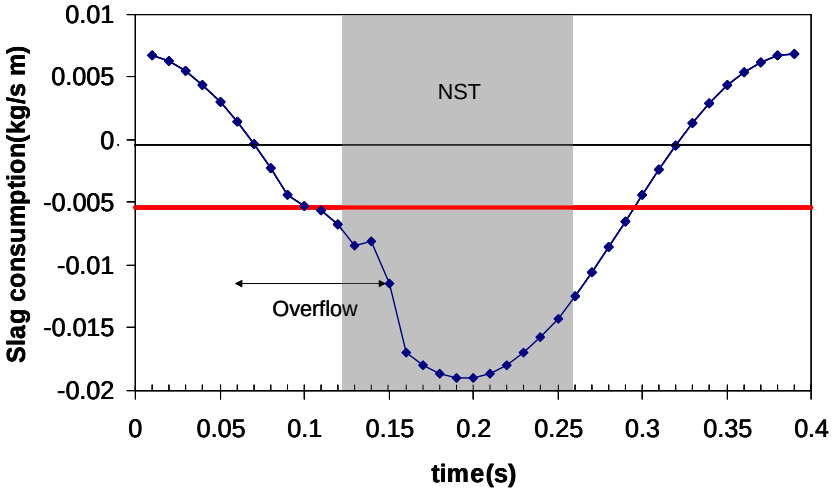

Fig. 20 Instantaneous and mean consumption of liquid slag into the gap

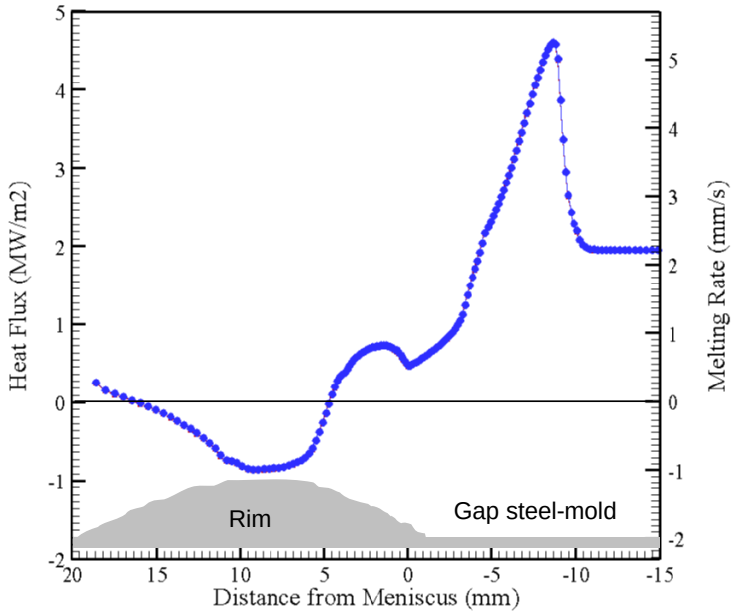

Fig. 21 Heat flow towards mold wall and solid flux layer / rim melting rate

CONCLUSIONS

A computational flow model has been developed to simulate transient behavior in the meniscus region during an oscillation cycle, including fluid flow and pressure evolution in the molten slag and molten steel, movement of the solid slag rim above the meniscus, movement of the steel-slag interface, meniscus overflow, slag consumption into the gap. The model predictions are validated through comparison with analytical solutions and plant measurements and are interpreted to provide insight into the mechanism of hook and oscillation mark formation. Specific findings are as follows.

1. The oscillating solidified slag rim controls the flow pattern in the meniscus region, so must be taken into account in the study and optimization of initial solidification phenomena.
2. Pressure in the gap between the shell and mold oscillates. Pressure increases during the negative strip period which moves the steel/slag interface away from the mold wall and decreases as the mold increases its upward velocity which pulls the interface against the mold.
3. For the assumptions and conditions of this model, the meniscus overflow event tends to start 1/6 of the oscillation cycle before negative strip starts, and finishes about 1/12 of the cycle into negative strip.
4. Computations and experimental data both show that the overflow event can start at different times during the oscillation cycle, which results in hooks of different shapes.
5. Liquid flux consumption varies during the oscillation cycle, occurring mainly during the negative strip period, but also is positive during part of the positive strip period. The mean consumption predicted by the model agrees well with that measured at the steel caster.
6. The heat flux peak occurs several mm below the meniscus level, owing to meniscus curvature.
7. The bottom part of the solid rim is predicted to melt back over several oscillation cycles (less than 1 minute) to reach a new equilibrium shape that is less severe than assumed in this work.
8. The range of meniscus shapes predicted during the oscillation cycle matches well with shapes of measured hooks. The slight extra curvature appearing in hook measurements might be due to thermal strain and requires further study.

ACKNOWLEDGEMENTS

The authors are grateful to Fundacion Labein – Tecnalia, Derio, Spain, the National Science Foundation (Grant DMI 05-28668), and the Continuous Casting Consortium at University of Illinois at Urbana-Champaign for support of this project, and to Fluent Inc., for supplying the FLUENT package.

REFERENCES

1. J. Sengupta, B.G. Thomas, H.-J. Shin, G.-G. Lee and S.-H. Kim, *"A new mechanism of hook formation during continuous casting of ultra-low carbon steel slabs,"* Metallurgical and materials transactions A, 2005.
2. B.G.Thomas, *"Slab casting phenomena,"* 2005, Continuous Casting Consortium Website.
3. H. Steinruck and C. Rudischer, *"Numerical investigation of the entrainment of flux into the lubrication gap in continuous casting of steel*," in *Fifth World Congress on Computational Mechanics*. 2002. Viena, Austria.
4. J.R. King, A.A. Lacey, C.P. Please, P. Wilmott and A. Zoryk, *"The formation of oscillation marks on continuously cast steel,"* Math. Engng. Ind., 1993. 4(2): p. 91-106.
5. E. Takeuchi and J.K. Brimacombe, *"The formation of oscillation marks in the continuous casting of steel slabs,"* Metallurgical Transactions B, 1984. 15B: p. 493-509.
6. C. Perrot, J.N. Pontoire, C. Marchionni, M.R. Ridolfi and L.F. Sancho, *"Several slag rims and lubrication behaviors in slab castings,"* in *European Continuous Casting Conference 2005*. 2005.
7. S. Takeuchi, Y. Miki, S. Itoyama, K. Kobayashi, K.-I. Sorimachi and T. Sakuraya, *"Control of oscillation mark formation during continuous casting,"* in *Steelmaking conference proceedings*. 1991.
8. R.B. Mahapatra, J.K. Brimacombe and I.V. Samarasekera, *"Mold behavior and its influence on quality in the continuous casting of steel slabs: Part II. Mold heat transfer, mold flux behavior, formation of oscillation marks, longitudinal off-corner depressions, and subsurface cracks,"* Metallurgical Transactions B, 1991. 22B: p. 875-888.
9. I.V. Samarasekera, *"Crack formation,"* in *Brimacombe Continuous Casting Course*, 2005. p. Secction R.
10. E. Takeuchi and J.K. Brimacombe M. Hanao, M. Kawamoto, T. Murakami and H. Kikuchi, *"Effect of oscillation-mark formation on the surf ace quality of continuously cast steel slabs,"* Metallurgical Transactions B, 1985. 16B: p. 605-625.
11. Y. Meng, B.G. Thomas, A.A. Polycarpou, H. Henein and A. Prasad. *"Mold slag measurements to characterize CC mold-shell gap phenomena,"* in *Materials Science & Technology 2004*. 2004. New Orleans, LA.
12. Y. Meng and B.G. Thomas, *"Heat transfer and solidification model of continuous slab casting: CON1D,"* Metallurgical Transactions B, 2003. 34B: p. 685-705.
13. M. Hanao, M. Kawamoto, T. Murakami and H. Kikuchi, *"Mold flux for high speed continuous casting of hypoperitectic steel slabs,"* in *European Continuous Casting Conference 2005*. 2005.
14. K.C. Mills and A. B. Fox, "*The role of mould fluxes in continuous casting-So simple yet so complex,"* ISIJ International, 2003. 43(10): p. 1479-1486.
15. S. McKay, N.S. Hunter, A.S. Normanton, V. Ludlow, P.N. Hewitt and B. Harris, *"Continuous casting mould powder evaluation,"* Ironmaking and Steelmaking, 2002. 29(3): p. 185-190.
16. K.C. Mills, A. B. Fox, and M.C. Bezerra, *"A logical approach to mould powder selection,"* in *MMT 2000*. 2000.
17. K.Schwerdtfeger and H. Sha, *Depth of oscillation marks forming in continuous casting of steel.* Metallurgical and Materials Transactions B, 2000. **31B**: p. 813-826.
18 H. Steinruck, C.Rudischer and W.Schneider, "*The formation of oscillation marks in continuous casting of steel*." in *Modeling of Casting, Welding and Advanced Solidification Processes VIII*. 1998: The Minerals, Metals and Materials Society.
19. J. Barco, M. Ojanguren, J. Palacios, M. Serna, C. Ojeda and V. Santisteban, *"Global modelization of continuous casting process,"* in European Continuous Casting Conference, 2005. Nize.
20. B.G. Thomas and F.M. Najjar, *"Finite element modelling of turbulent fluid flow and heat transfer in continuous casting,"* Applied Mathematical Modeling, 1991. 15: p. 226-243.
21. Y. Meng and B.G. Thomas, *"Modeling transient slag layer phenomena in the shell/mold gap in continuous casting of steel,"* Metallurgical and materials transactions B, 2003. 34B: p. 707-725.
22. R.M. McDavid and B.G. Thomas, *"Flow and thermal behavior on the top surface flux/powder layers in continuous casting molds,"* Metallurgical and materials transactions B, 1996. 27B: p. 672-685.
23. C.A. Pinheiro, I.V. Samarasekera and J.K. Brimacombe, *"Mold flux for continuous casting of steel,"* in *I&SM*. 1994 - 1995 - 1996.
24. J. Sengupta and B.G. Thomas, *"Visualization of hook and oscillation mark formation mechanism in ultra-low carbon steel slabs during continuous casting,"* JOM-e(TMS), 2005: p. 1-21.
25. E. Anzai, T. Ando, T. Shigezumi, M. Ikeda and T. Nakano, *"Hydrodynamic behavior of molten powder in meniscus zone of continuous casting mold,"* 1987, Nippon Steel. p. 31-40.
26. J. Sengupta, H.-J. Shin., B.G. Thomas and S.-H. Kim, "Micrograph evidence of meniscus solidification and sub-surface microstructure evolution in continuous-cast ultra-low carbon steels," Acta Materiala, 2005.
27. H.-J. Shin, G.-G.Lee., S.-M. Kang, S.-H. Kim, W.-Y. Choi, J.-H. Park, and B.G. Thomas, "*Effect of mold oscillation on powder consumption and hook formation in ultralow-carbon steel slabs,"* Iron and Steel Technology, 2005: p. 56-69.
28. .K. Tsutsumi, J.-I. Ohtake and M. Hino, *"Inflow behavior observation of molten mold powder between mold and solidified shell by continuous casting simulator using Sn-Pb alloy and stearic acid,"* ISIJ International, 2000. 40(6): p. 601-608.
29. B. Zhao, S.P. Vanka and B.G. Thomas, *"Numerical study of flow and heat transfer in a molten flux layer,"* International Journal of Heat and Fluid Flow, 2005. 26: p. 105-118.
30. S. Furuhashi, M. Yoshida, and T. Tanaka: *Tetsu-to-Hagane*, **84** (1998), pp. 625-631.